3-D Disks Using Photopolymer Films

Kevin Curtis

Northrop B-2 Division, Pico Rivera, Ca. 90660, and
California Institute of Technology, Dept. of Electrical Eng., 116-81, Pasadena, Ca. 91125.

Allen Pu, Hsin-Yu Li, and Demetri Psaltis

California Institute of Technology, Dept. of Electrical Eng., 116-81, Pasadena, Ca. 91125.

ABSTRACT

The recording characteristics of DuPont's HRF-150 photopolymer film are described. The application of these films for data storage using the 3-D holographic disk architecture is presented. The required system's bandwidth due to the photopolymer's limited thickness is shown to be the limiting factor of the storage capacity of these thin films and not the material's dynamic range. A new multiplexing method (peristrophic multiplexing) that significantly increases the film's capacity and changes the limiting factor from system bandwidth to material dynamic range is presented.

2. INTRODUCTION

DuPont's HRF-150 photopolymer film is investigated for use in 3-D holographic memories. In particular, 3-D holographic disk systems are of interest because they can be used as memories and correlation devices with very high storage density and correlation rates[1,2,3]. DuPont's HRF-150 photopolymer has excellent sensitivity and good resolution for transmission holograms recorded with blue-green light.[4,5,6] Thus it is a likely candidate for use as a holographic storage material. This paper presents results on sensitivity, hologram persistence, the lateral spread of the photo-initiated reaction, and the variation of the diffraction efficiency with modulation depth, spatial frequency/tilt angle and intensity. These are all important characteristics for evaluation of these photopolymer films as media for holographic storage applications. In addition, this paper present angle multiplexing results[7], and a new multiplexing method (peristrophic multiplexing) that signicantly increases the storage capacity of thin films.

3. RECORDING CHARACTERISTICS FOR A SINGLE GRATING

HRF-150 photopolymer films consist of 38μm thick photopolymer film sandwiched between two thin sheets of mylar. Hologram storage was performed using the setup shown in Figure 1. The object beam is incident normal to the surface, while the reference beam is incident at an angle θ. Both beams are plane waves at 488 nm and the film is mounted on a glass substrate. After recording, the hologram is fixed by exposing the film to uniform UV light for 45 seconds. We define diffraction efficiency as incident intensity divided by diffracted intensity after the reference beam is re-Bragg matched to adjust for film shrinkage[8].

The sensitivity curve of the material was measured by plotting the diffraction efficiency of the first diffracted order against the total exposure energy. The intensity of each beam was kept constant at 2 mW/cm^2 with $\theta \approx 18°$ and the exposure time varied to vary the exposure energy. When the diffraction efficiency exceeded 20%, a considerable amount of energy was diffracted into the 2 and -1 orders. The saturation exposure was approximately 80 mJ/cm^2 and it took about 15 mJ/cm^2 to get into the linear recording regrime.

We also measured the effect of the intensity on the photopolymer's sensitivity. Keeping the

0-8194-1447-6/94/$6.00

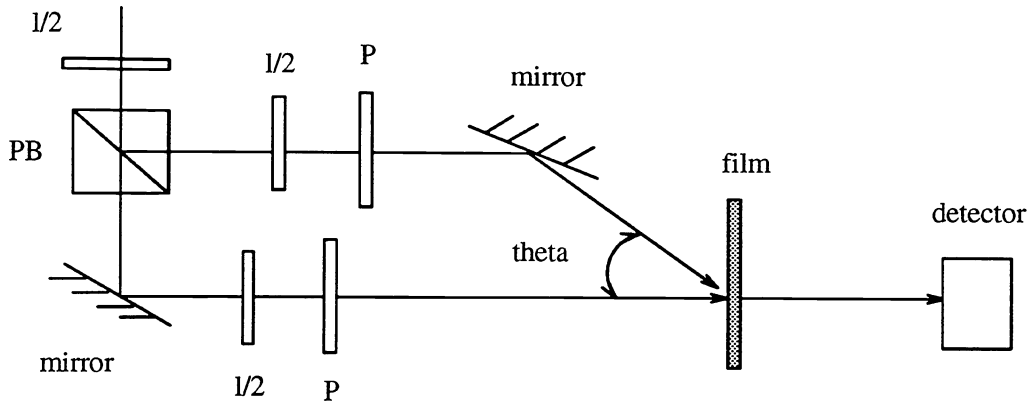

Figure 1: Recording Geometry used for measurements with the elements given as: P – polarizer, 1/2 – half-wave plate, PB – polarizing beam splitter.

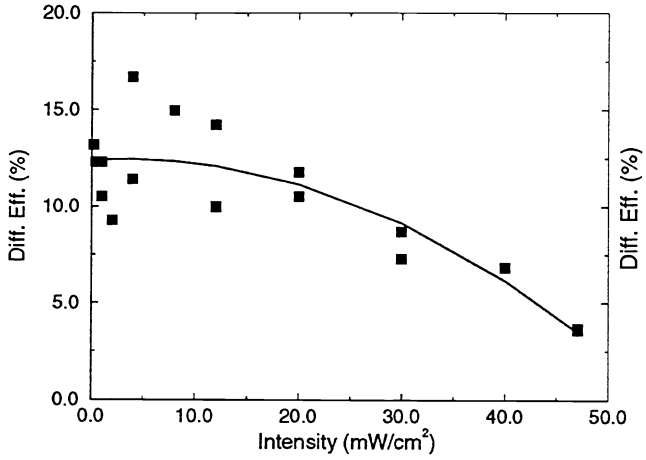

Fig. 2: Diff. eff. vs Int. for E = 20 mJ/cm^2.

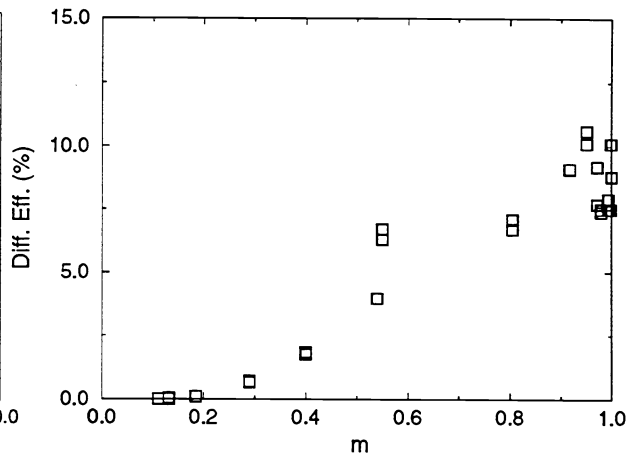

Fig. 3: Diff. Eff vs m.

intensities of the two beams equal, $\theta \sim 20°$, and the total exposure of 20 mJ/cm^2, the diffraction efficiency was measured as the total intensity of the two beams was changed. Figure 2 shows that as the intensity is increased, the film becomes less effective. Since the photo-initiated reaction is a free radical reaction, it can be slowed or stopped by inhibitors. Free radicals themselves are very efficient inhibitors, therefore, increasing intensity, which generates more free radicals, can inhibit the reaction.

The modulation depth is defined as $m = 2RS/(R^2 + S^2)$ where R and S are the amplitudes of the reference and the signal beams. Figure 3 shows the diffraction efficiency versus m for $\theta \sim 20°$ with the total exposure kept constant at 20 mJ/cm^2. The curve shows that if $m < 0.2$, the diffraction efficiency is small. This is probably due to the fact that at low modulation the large background intensity polymerizes the material uniformly which impedes monomer diffusion. The curve also shows a saturation behavior around $m = 1$. This saturation is not due to the normal diffraction from a strong grating because we have a relatively weak modulation ($\frac{2\pi\Delta nL}{\lambda n} < .33$). Therefore, we attribute this saturation to the monomer diffusion mechanism in the film.

The film's response to grating frequency is measured by recording the diffraction efficiency as a function of the angle between the beams while keeping the bisector of the angle perpendicular

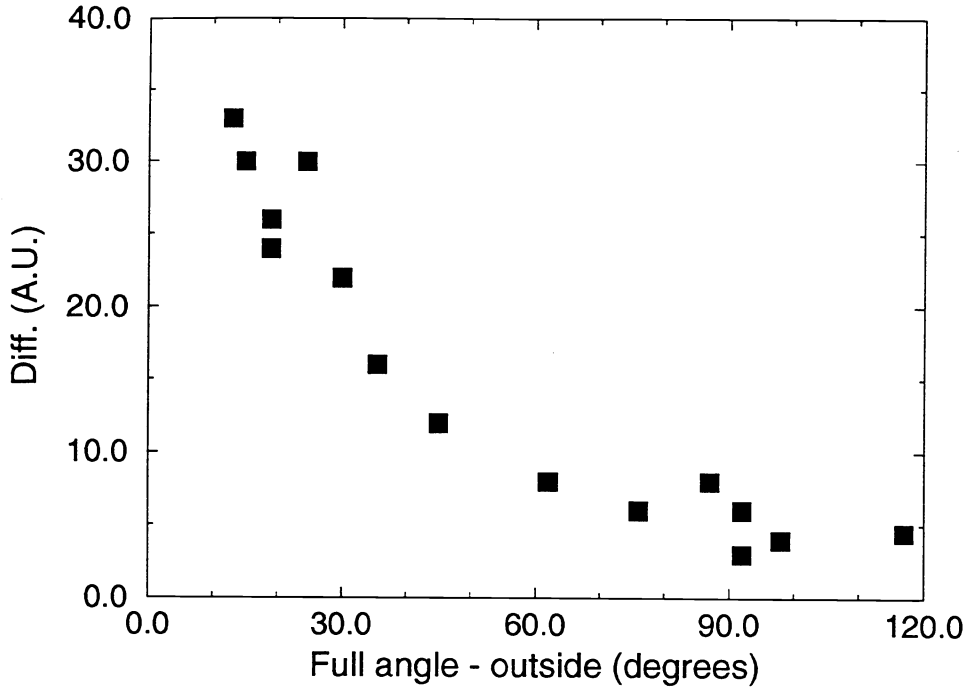

Figure 2: Diffraction efficiency vs full angle between the beams outside the material for E = 20 mJ/cm^2 and no grating tilt.

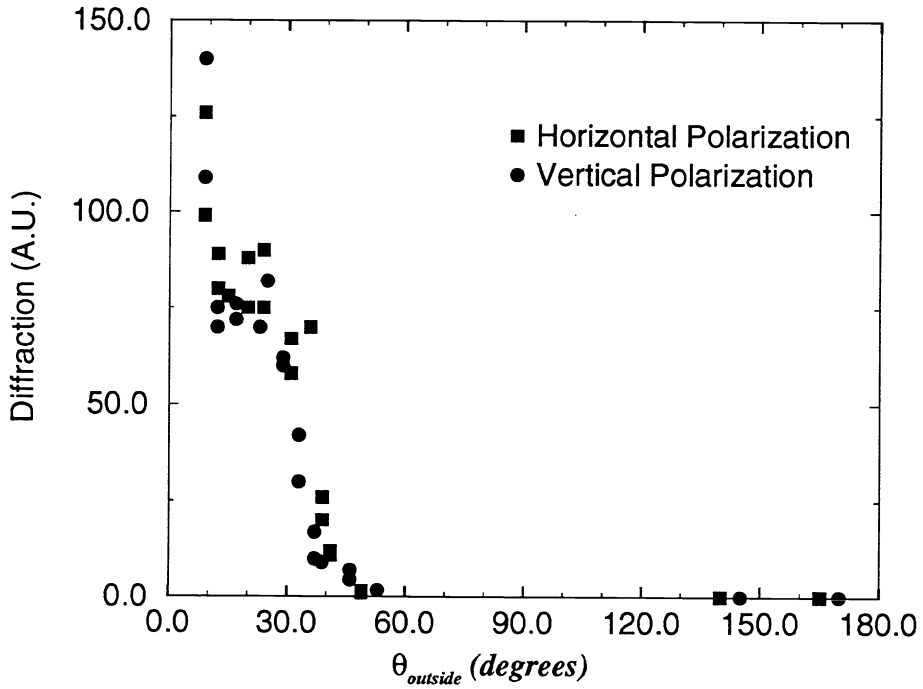

Figure 3: Diffraction efficiency vs angle outside the material for E = 20 mJ/cm^2 image beam incident normal to the surface.

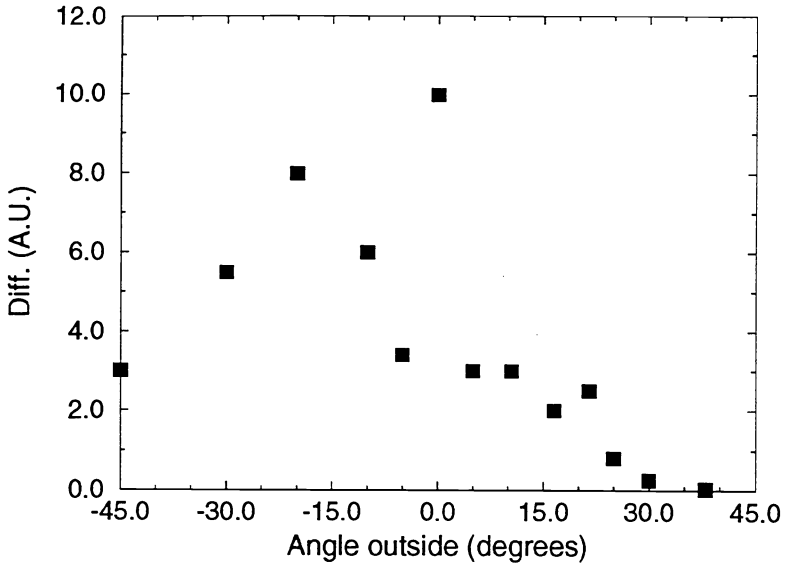

Figure 4: Diffraction efficiency vs angle outside the material for E = 20 mJ/cm^2 with 90° degrees between the 0° reference beam and the signal.

to the film's surface. This geometry ensures that the fringes are always perpendicular to the film surface. Figure 2 shows the result for $E = 20$ mJ/cm^2. The efficiency is plotted against the full angle between the beams to make it easier to understand the next two results. Notice that the film prefers lower frequency gratings but the curve becomes flatter around 90° between the beams. The 3db point of the frequency response is at approximately 30°, corresponding to approximately 1,000 cycles/mm.

Figure 3 shows the diffraction efficiency for a total exposure of 20 mJ/cm^2 as a function of the reference angle θ for both polarizations with the signal beam incident normal to the surface. The intensity of each beam is 2.2 mW/cm^2. The results for each polarization are similar. HRF-150 is designed by DuPont as a transmission film and, as Figure 2 shows, it does not effectively record reflection holograms. Comparing this result with Figure 2, we see that the drop in efficiency for angles larger than 30° is not due entirely to the change in spatial frequency. It appears that the film does not effectively record gratings that have a large tilt angle inside the material. This is probably due to the film's thickness being only 38μm.

To evaluate this effect further, we again measured the film's response as the reference angle is changed, but this time with the center angle between the beams being 90° where we know (from Figure 2) that the film's frequency response is relatively flat. Figure 4 plots diffraction efficiency for a total exposure of 20 mJ/cm^2 as a function of the reference angle θ. In this plot, an angle of 0° refers to 90° angle between the beams with no tilt in the gratings. Notice that at -45° the diffraction is less than at -20° even though we know that the spatial frequency at -45° is preferred by the film when the grating is not tilted. This loss in sensitivity is attributed to the grating tilt. The maximum fringe tilt that the film can tolerate is approximately 10°.

If the material is going to be used as a storage element, the holograms must be able to be recalled nondestructively after they are fixed with UV light. A single hologram has been reconstructed for 100 hours. The reference intensity was $\sim$ 3mW/cm^2 with a diffraction efficiency of about 1.5%. There was an initial increase in diffraction efficiency that was due to the bleaching of the material with light exposure. The grating was recorded with the object beam incident at -45° and the reference beam incident at 45° from surface normal. Multiplexed image plane holograms recorded more than a year ago and stored at room temperature can still be recalled.

Whether or not the reaction spreads laterally (in the plane of the film) is important if spatial

multiplexing is desired. To test if the reaction spreads, a slit about 1mm across and 1cm long was cut in tin-foil to create a mask. The photopolymer was exposed with a single normal incident beam through this mask (E$\approx$ 300mJ/cm^2). The sample was then left in the dark, giving the reaction time to polymerize the material in the exposed region and possibly laterally spread to beyond the illuminated area. The mask was then removed and a hologram recorded in a large area around the slit's location on the film. The reconstructed hologram consists of bright areas where the film was unaffected by the first exposure, and dark areas where the film had already been exposed. Any lateral spreading of the reaction would cause a gradual loss of efficiency as the reaction spreads out and uses up the film's dynamic range. When the second exposure immediately followed the first, no appreciable lateral spread was observed. The experiment was repeated, except this time the sample was left in the dark for 16 hours before the holographic exposure was done. Again, a dark slit was seen in the hologram with no noticeable lateral spread. Therefore, within a measurement error of $\sim 100\mu$m, the reaction does not laterally spread.

4. RECORDING OF MULTIPLE HOLOGRAMS IN PHOTOPOLYMER FILMS

A sheet of DuPont HRF-150 photopolymer was taped to a glass plate with a centered window cut out of it and mounted on a rotation stage. The holograms were recorded with visible light($\lambda = 488nm$) with 90 degrees between the writing beams and then fixed with UV light. First the angular selectivity of the material was determined at 488 nm. The material was approximately 38 microns thick, and had angular selectivity (half width, measured at the first minimum) of one degree in very good agreement with Kogelnik's two wave theory[9] for diffraction from thick phase gratings. First, this indicates that the gratings are not due to surface deformations which has been observed in similar materials for low spatial frequency holograms. Also it indicates that the recorded hologram is most likely a phase grating rather than an absorption grating since the diffraction efficiency of 17.1 percent would be too large for an absorption grating.

Diffraction efficiency for 10 holograms of the same image stored at 10 different angular setting of the recording medium while keeping the angles between the recording beams the same was measured. The holograms were recorded at intervals of two degrees or at the second minima of the angular selectivity curve of the adjacent holograms. The holograms were read out by blocking the object beam and detecting the reconstructed image while rotating the sample. This resulted in the first two holograms (at $-10°$ and $-8°$) being weaker than the others, which indicates that exposure to light enhances the sensitivity.

Figure 5 shows 10 image holograms of roughly equal strength that were recorded with a five second pre-illumination pulse with 1.85 mW/cm^2 intensity ten seconds before the first hologram was recorded. Both experiments used the same setup, and, except for the pre-illumination pulse, identical recording parameters were used. The total recording energy per hologram was 1.88 mJ/cm^2 (one second exposure per hologram) with an object-to-reference beam ratio of approximately 1/4.6. The time between holograms is 10 seconds for a total experiment run time of 120 seconds. The diffraction efficiency shown is calculated by dividing the diffracted light by the incident minus reflected light intensities, and multiplied by 100 to convert to a percentage. The pre-illumination pulse sensitizes the material and is necessary if the first hologram is to be recorded effectively. Since the material has a finite dynamic range, too long of a pre-illumination pulse wastes dynamic range causing the later holograms to be weaker than previous ones. Too short of a pre-illumination pulse fails to sensitize the material and the first few holograms are lost.

The index perturbation was calculated by measuring the Bragg matched diffraction efficiency and solving for Δn as in reference 9. In this case the diffraction efficiency used for η is diffracted light divided by transmitted light intensity to eliminate the effects of reflection from the surface and absorption. Notice also that the saturation exposure was about 20 mJ/cm^2; therefore, each of the ten holograms should be given about 2 mJ/cm^2. This is close to the actual value of 1.88 mJ/cm^2 per hologram used. Without the pre-illumination pulse the maximum Δn obtained was $\Delta n \approx .0028$. The Δn we measured is lower than what is reported in reference 10 ($\Delta n \approx .008$), most likely

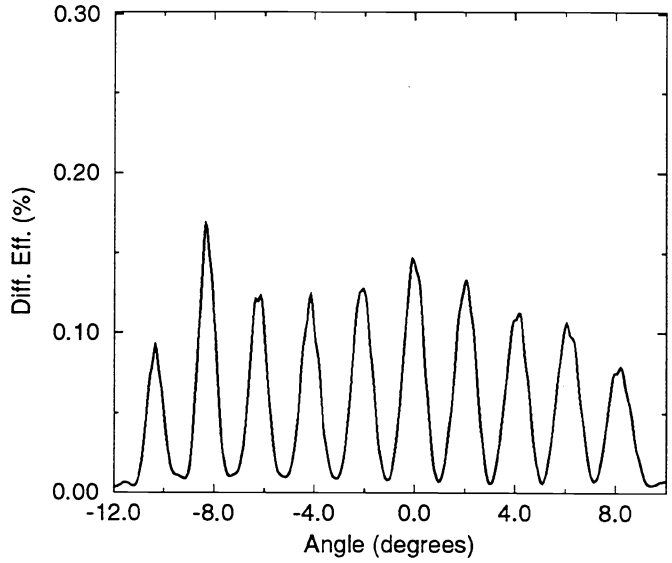

Figure 5: 10 Image Plane Holograms.

because of the much higher spatial frequency recorded in out experiment (2897 cycles/mm versus 1007 cycles/mm). With the pre-illumination pulse, the saturation exposure for this material is 20 mJ/cm^2 for a $\Delta n_{max} = 1.7 \times 10^{-3}$. In comparison, for a thick sample of $BaTiO_3$ [10] the experimentally measured saturation exposure is approximately 100 mJ/cm^2. Recent experiments with thin samples of $BaTiO_3$[11] and doped SBN [12] indicate sensitivities and Δn's roughly equivalent to the photopolymer.

Figure 6 shows the effect of extending the total run time by increasing the time between holograms from 10 seconds as in Figure 5 to one minute. As the exposure time increases the dynamic range of the material is also used up as the residual monomer is polymerized. The decrease in hologram strength due to loss of dynamic range is evident in Figure 6. Therefore, not only is angular selectivity and exposure time important parameters for recording, but total run time is also. In order to maximize the number of holograms that can be stored, the total run time (T_{run}) should be minimized. T_{run} depends on t_{setup} (the time to present an image to the system and change the angle) and t_e (the exposure time) which varies as t_o/N where t_o is the single hologram saturation time and N the number of holograms. T_{run} can be written as

$$T_{run} = t_{setup} \times N + t_e \times N = t_{setup} \times N + t_o. \quad (1)$$

Using N=1000, $t_{setup} = .1$ seconds, and $t_o = 10$ seconds results in a total run time of 110 seconds. For a large number of holograms , the setup time dominates t_o. However since t_{setup} can be equal to .1 seconds or less, the total run time even for 1000 holograms is below the 120 seconds that was experimentally demonstrated. Therefore, in practice the total run time is not the limiting factor in the number of holograms that can be stored.

The factor that does limit the number of holograms that can be stored is the thickness of the current samples. Increasing the thickness of the material, increases the angular selectivity and hence the storage capacity of the material. As an example, let us assume that we can fabricate material that is 4 mm thick with sufficiently low scatter level. Then using the method presented in Reference 13 and with a maximum index perturbation of $1x10^{-3}$, we predict that around 2,800 holograms each with .01 percent diffraction efficiency can be superimposed in this material. However fabricating thick samples with good optical quality is not trivial. All methods tried so far have resulted in a rapid increase in scattering with any increase in thickness. Thus, scattering limits the maximum useful thickness of the material.

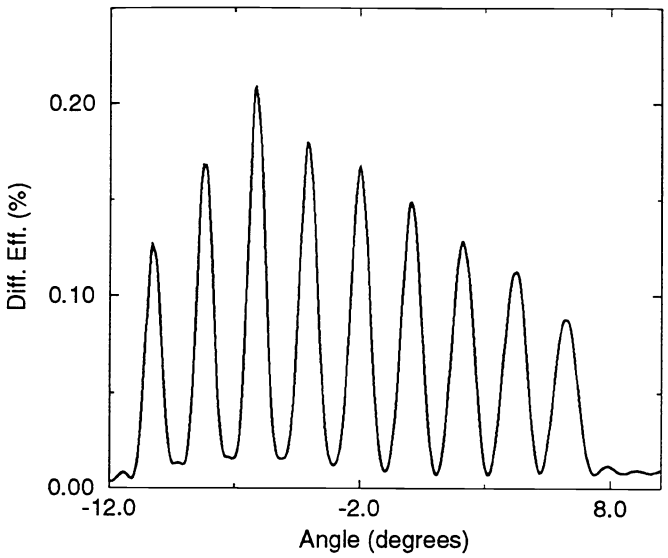

Figure 6: 10 Image Plane Holograms, 1 minute apart.

5. 3-D DISKS FOR DATA STORAGE

Holographic storage of data in 3-D materials such as photorefractives or photopolymers can provide large capacities and fast parallel readout of the stored information. These memories were investigated in the 1960's and 1970's, but they never found commercial applications. Recently, with improvements in materials, light sources, detectors, and the invention of spatial light modulators holographic storage has again arisen as a possible mass storage candidate. The theoretical upper limit on the storage density is V/λ^3, where V is the volume of the media and λ is the wavelength of the light used. This limit suggests that densities of $\sim 10^{12}$ bits per cm^3 are possible. Unfortunately, due to the finite numerical aperture or the finite dynamic range of the material, practical systems are limited to approximately 10^9–10^{10} bits per cm^3. For example, 10^3 holograms each with 10^6 pixels has a total capacity of 10^9 bits. With the increase in the storage densities of both magnetic and RAM memories, storage technologies that are limited to these capacities are not of practical use. In order to increase the capacity to useful levels it is necessary to spatial multiplex the holograms as well as volumetrically multiplexing them. Spatial multiplexing simply means to use new, "unexposed" material to record more holograms.

The system presented here accomplishes the spatial multiplexing by shaping the medium in the form of a disk and rotating the disk or move the location of the beams. At each spot on the holographic disk (HD), holograms are multiplexed by changing the angle of the reference beam. The disk/head motion is used to access new spots to record the information just like in the correlator in the preceding section. To get the data out, the correct plane wave reference is to illuminated the correct spot on the disk. Figure 7 shows a disk system were holograms are multiplexed in either transmission or reflection geomerties. In this section, we present the geometrically limited storage capacity of such a system for an angle multiplexed HD. The derivation follows the derivation presented in reference 3 where the signal beam is incident normal to the disk surface. Figure 8 shows the resulting density vs film thickness. Figure 8 was calculated with λ=488nm, 10° sweep of the reference beam inside the medium, 10^6 bits per hologram, $n = 1.525$ and $F^{\#} = 1$ optics. Notice that for a 40μm thick film the optimal number of angle multiplexed holograms is about 20 holograms/spot. Therefore, our demonstrated 10 angle multiplexed holograms would work out to about 6 bits/μm^2. Clearly, increasing the number of holograms that can be stored at one location has important consequences for storage densities.

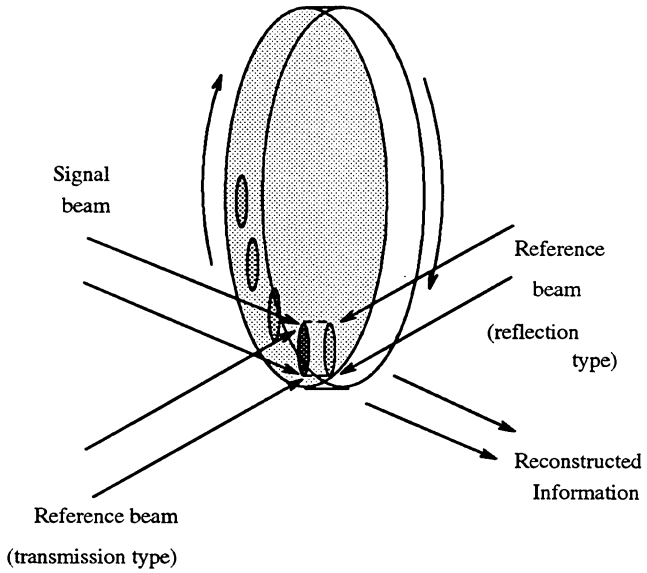

Figure 7: Using the disk as a storage device by presenting the reference plane wave for reconstruction of the stored data.

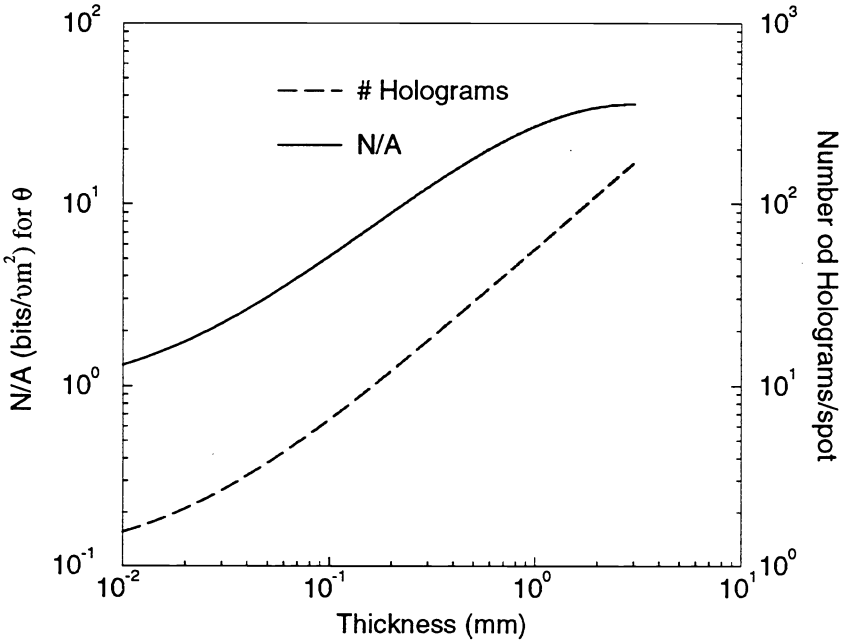

Figure 8: Geometrical storage limit of angle multiplexed HD.

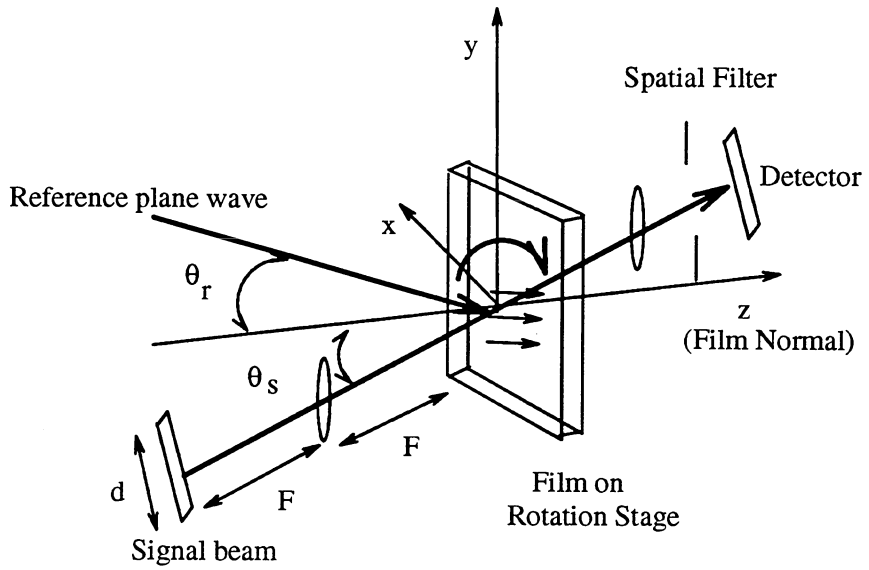

Figure 9: Setup for peristrophic multiplexing.

6. PERISTROPHIC MULTIPLEXING

The number of holograms that can be multiplexed in a given holographic system is primarily a function of two parameters – the system's bandwidth (either temporal or spatial frequency) and the material's dynamic range. A previous section reported 10 angle multiplexed holograms in a 38μm thick film with diffraction efficiency of 10^{-3}. Since we can typically work with holographic diffraction efficiencies on the order of 10^{-6}, we have sufficient dynamic range to record significantly more than 10 holograms. The angular bandwidth limitation can be alleviated by making the film thicker but scattering increases rapidly with thickness in these materials. Another method that has been previously used to increase the utilization of the available bandwidth of the system is fractal sampling grids[14,15].

In this section we describe peristrophic (consisting of turns) multiplexing as a solution to the bandwidth limited capacity problem. With this method the hologram is physically rotated with the axis of rotation being perpendicular to the film's surface every time a new hologram is stored. The rotation does two things. It shifts the reconstructed image away from the detector allowing a new hologram to be stored and viewed without interference, and it can also cause the stored hologram to become non-Bragg matched.

6.1 Theory

The setup for peristrophic multiplexing is shown in Figure 9. The reference plane wave (R) is incident at an angle θ_r and the signal beam (S) is incident at an angle θ_s, both angles measured with respect to the film's normal. Taking the center pixel of the image as the signal and neglecting any effects due to hologram thickness, the hologram transmittance can be written as

$$R^* S = e^{-i2\pi \frac{\sin\theta_r}{\lambda} x} e^{-i2\pi \frac{\sin\theta_s}{\lambda} x} \tag{2}$$

The hologram is then rotated by $d\theta$ about the center of the x-y plane as shown in Figure 1. Assuming the rotation is small, this results in the coordinates being tranformed according to: $x' \approx x - yd\theta$, and $y' \approx y + xd\theta$. Substituting these into Eq. 2, the hologram be expressed in terms

of the unrotated coordinates (x, y)

$$R^* S = e^{-\frac{2\pi \sin\theta_r x}{\lambda}} e^{\frac{-2\pi \sin\theta_s x}{\lambda}} e^{\frac{-2\pi(\sin\theta_s + \sin\theta_r)d\theta y}{\lambda}}. \tag{3}$$

After Fourier tranforming, the last term in Eq. 3 is a shift in the image. The rotation required to translate the image out of the detector aperture is approximately given by,

$$d\theta \geq \frac{\frac{d}{F}}{\sin\theta_s + \sin\theta_r}, \tag{4}$$

where d is the size of the image at the detector plane and F is the focal length of the lens used. For image plane holograms with the signal beam at normal incidence, the expression is

$$d\theta \geq \frac{\frac{2\lambda}{\delta}}{\sin\theta_r}, \tag{5}$$

where $1/\delta$ is the highest spatial frequency in the image. Notice that this method can be combined with other volumetric multiplexing methods to further increase the storage capacity.

The Bragg selectivity, assuming the reference is given by $R = e^{-i(\frac{2\pi \sin\theta_r}{\lambda}x + \frac{2\pi \cos\theta_r}{z})}$ and the signal given by $S = e^{i(\frac{2\pi \sin\theta_r}{\lambda}x + \frac{2\pi \cos\theta_r}{z})}$, can be calculated using the Born and paraxial approximations and integrating over the volume. Assuming that the tranverse (x, y) dimensions of the film are much larger than the bandwidth of the images and $\theta_s \gg 0$, the Bragg selectivity can be shown to be

$$d\theta = \sqrt{\frac{2\lambda}{t\cos\theta_s}}\left(\frac{1}{\sin\theta_s + \sin\theta_r}\right), \tag{6}$$

where t is the thickness of the material. Using $\lambda = 488$nm, $t = 38\mu$m, and $\theta_s = \theta_r = 30°$ results in a selectivity of about 9°. The Bragg matching requirement is the dominant effect if $\frac{d}{F} < \sqrt{2\lambda/t\cos\theta_s}$. For most material thicknesses, the Bragg matching criterion determines the required rotation for peristrophic multiplexing. In our experiments, because the thickness of the film is only 38μm, the image could be filtered out before the gratings become non-Bragg matched.

6.2 Experimental Results

The experimental setup is the same as in Fig. 9 except a rotation stage was added to rotate the film around a vertical axis as well as around the film's normal. This makes it possible to combine peristrophic and angle multiplexing. The film was located a significant distance from the Fourier plane so that the siganl beam was approximately uniform. For each peristrophic position, multiple holograms are stored using standard angle multiplexing by rotation the medium. A spatial light modulator (SLM) was used to present images (cartoons) to the system. Each frame is numbered according to the sequence in which they were stored. The reference and signal beams were initially incident at $\pm 30°$ from the film's normal. The reference beam intensity was 1.1 mW/cm^2 and the signal beam had 300 μmW in about a 1 cm by 0.5 cm area. The film was rotated in-plane by 3° between each set of rotation (angle) multiplexed holograms to enable the other holograms to be filtered out. Eq. 3 predicts a required rotation of about 9° for Fourier plane hologram while Eq. 4 predicts about 1.7° rotation for image plane. The 3° was experimentally obseved for the in-between (fresnel) case we used. Each rotation (angle) multiplexed hologram was also separated by 3°. The initial exposure time was 0.11 seconds, but starting at hologram number 26, each hologram was exposed for 0.005 seconds longer than the previous hologram to correct for the lost sensitivity due to run time. There was a 1.5 second delay between holograms to allow the rotation stages to

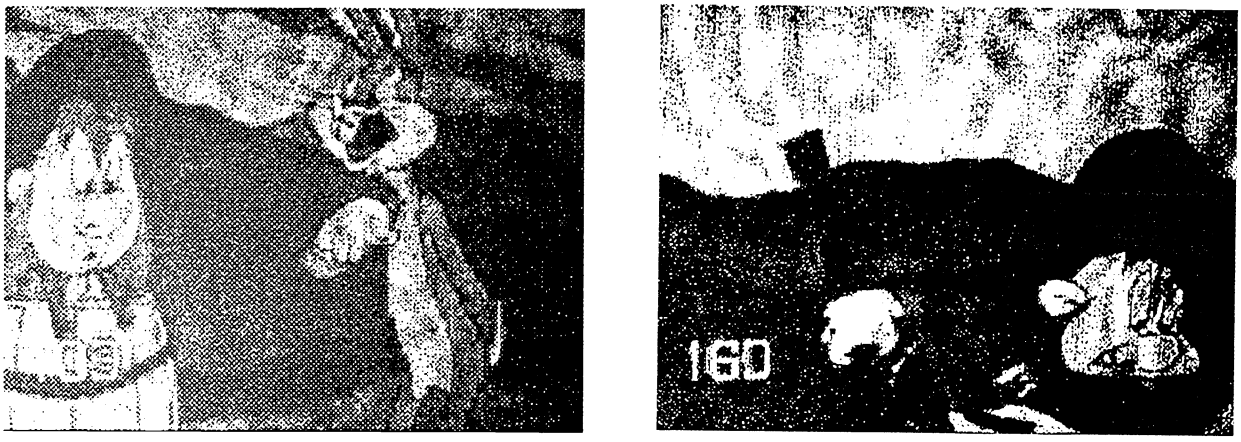

Figure 10: Examples of the 295 reconstructed holograms.

completely stop. Fig. 10 shows three of the 295 holograms stored in the polymer by peristrophic multiplexing 59 times and storing 5 angle multiplexed holograms with each peristrophic position. The average diffraction efficiency of the 295 holograms was $\sim 4 \times 10^{-6}$.

7. CONCLUSIONS

In summary, we have observed that the sensitivity of the HRF-150 photopolymer decreases with an increase in recording intensity and an increase in grating tilt angle. The holograms can be nondestructively reconstructed for long periods of time at room temperature. The photo-initiated reaction was seen to spread less than 100μm over periods of many hours. Overall, the HRF-150 has many of the desirable characteristics needed for a practical holographic storage material. The major improvement that is needed is an increase in film thickness to 200 μm or more. This would allow more holograms to be multiplexed at a single location and also it would probably alleviate the problem with tilted gratings that is reported in this paper. Previously we stored M =10 holograms with roughly 10^{-3} diffraction efficiency limited by the angular bandwidth of the optical system. Peristrophic multiplexing made it possible to store M =295 holograms with a diffraction efficiency of $\sim 4 \times 10^{-6}$. The loss in diffraction efficiency is approximately consistent with the $1/M^2$ decrease in diffraction efficiency that is theoretically expected[16]. Thus, peristrophic multiplexing allowed for almost two orders of magnitude increase in the storage capacity of the DuPont photopolymer and changed the limiting factor from the angular bandwidth of the optical system to the dynamic range of the material. By combining peristrophic and other multiplexing methods, it may be possible to achieve useful storage densities in these films; and, by using these films in the form of 3-D disks, high density data storage systems may be built.

8. ACKNOWLEDGEMENTS

We wish to thank Dr. Steve Zager of DuPont and Geoffrey Burr for their helpful discussions. This work was funded at Caltech by the AFOSR. Kevin Curtis gratefully acknowledges the support of the Northrop Fellowship program.

9. REFERENCES

1. D. Psaltis, "Parallel optical memories",*Byte*, 17(9):179–182 ,1992.

2. K. Curtis and D. Psaltis,"Multi-channel disk-based optical correlator," *SPIE Conference on Information Processing*, July 1993.

3. H. Y. S. Li, and D. Psaltis,"Storage Capacity of 3-D Holographic Optical Disks", accepted by *Applied Optics.*

4. W. K. Smothers, T. J. Trout, A. M. Weber, and D. J. Mickish,"Hologram recording in DuPont's new photopolymer material," *2nd Int. Conf. on Holographic Systems*, Bath, UK (1989).

5. A. M. Weber, W. K. Smothers, T. J. Trout, and D. J. Mickish,"Hologram recording in DuPont's new photopolymer materials," *SPIE Conference on Practical Holography IV*, Vol. 1212:30–39, 1990.

6. W. J. Gambogi, W. A. Gerstadt, S. R. Mackara, and A. M. Weber,"Holographic transmission elements using improved photopolymer films," *SPIE Conference on Computer and Optical Generated Holographic Optics*, Vol. 1555:256–267, 1991.

7. K. Curtis and D. Psaltis,"Recording of multiple holograms in photopolymer films," *Applied Optics*, 31:7425, 1992.

8. U. Rhee, H. J. Caulfield, J. Shamir, C. S. Vikram, and M. M. Mirsalehi,"Characteristics of the DuPont photopolymer for angularly multiplexed page-oriented holographic memories," *Optical Engineering*, 32(8):1839–1847, 1993.

9. H. Kogelnik,"Coupled wave theory for thick hologram gratings," *The Bell System Technical Journal*, 48(9):2909–2947, 1969.

10. J. Feinberg, D. Heiman, A. R. Tanguay, Jr., and R. W. Hellwarth,"Photorefractive effects and light-induced charge migration in barium titanate," *Journal of Applied Physics*, 51:1297-1305, 1980.

11. M. H. Garrett, J. Y. Chang, H. P. Jenssen, and C. Warde,"High photorefractive sensitivity in an n-type 45deg -cut $BaTiO_3$ crystal," *Optics Letters*, 17:103-5, 1992.

12. R. A. Vazquez, F. R. Vachss, R. R. Neurgaonkar, and M. D. Ewbank,"Large photorefractive coupling coefficient in a thin cerium-doped strontium barium niobate crystal," *Journal of the Optical Society of America B*, 8:1932-41, 1991.

13. J. Hong, P. Yeh, D. Psaltis, and D. Brady,"Diffraction efficiency of strong volume holograms", *Optics Letters*, 15: 344-346, 1990.

14. D. Psaltis, D. Brady, X. G. Gu, S. Lin,"Holography in artificial neural networks," *Nature*, 343(6256):325-330, 1990.

15. F. H. Mok,"Angle–multiplexed storage of 5000 holograms in lithium niobate," *Optics Letters*, 18(11):915–917, 1993.

16. D. Brady and D. Psaltis,"Control of volume holograms,"*Journal of the Optical Society of America A* 9(7):1167–1182, 1992.